Reachable Set Calculation and Analysis of Microgrids with Power-electronic-interfaced Renewables and Loads

Yan Li*, Peng Zhang†
Department of Electrical and Computer Engineering
University of Connecticut, Storrs, Connecticut 06269–4157
Emails: *yan.7.li@uconn.edu, †peng.zhang@uconn.edu

***Abstract*—A stability assessment approach via reachable set calculation is presented to efficiently evaluate the dynamics of microgrids. Due to their low inertia, microgrids are sensitive to the uncertainties introduced by power-electronic-interfaced renewables and loads. Through the reachable set-based method, the bounds of all possible trajectories of a microgrid under a series of disturbances can be directly obtained, which makes repeated traditional time-domain simulations unnecessary. Moreover, a zonotope is used to better quantify these uncertainties and is integrated into the reachable sets calculation procedure. Extensive testing shows that reachable set calculations enable an efficient analysis of disturbances impacts on a microgrids dynamics, as well as offer a potent tool for evaluating how far the system is from its stability margins and what actions should be taken by system operators. These salient features make reachability analysis a powerful tool for planning, designing, monitoring and operating future microgrid systems.**

***Index Terms*—Reachable set, stability, uncertainties, renewables, power-electronics interface.**

I. Introduction

Microgrids are being impacted by the increasingly deep integration of power-electronic-interfaced distributed renewables and power loads [1], [2]. On the one hand, distributed renewables alleviate or even prevent power outages locally because of their capability to operate autonomously; as such, significantly enhance electricity resiliency for customers. Meanwhile, power electronic interfaces offer customers a more flexible way to use electric power. On the other hand, most renewables and DC power loads need low-inertia power electronic devices to be integrated into a microgrid [3]. These interfaces make the microgrid highly sensitive to disturbances such as intermittent generations from photovoltaics (PV) or wind, and episodic loads produced by the plugin of hybrid electric vehicles. Therefore, understanding and quantifying the impact of a virtually infinite number of uncertainties (disturbances) on the transient stability of power-electronics-dominated microgrids is fundamentally important for planning, designing and operating.

There exist two major categories of dynamic assessment methods: time domain simulation and direct methods [4], [5], which can be applied in microgrids as well. The former approach computes the trajectories of state variables based on a specified system structure and initial condition [6]. This approach is known to be inefficient in handling parametric or input uncertainties. Even with Monte Carlo runs, it is still impossible to verify the infinitely many scenarios that can happen in a real system [7]. Direct methods can compute regions of attraction unattainable through time domain simulations and can be used to quickly check if control actions are capable of stabilizing systems. However, it is difficult to construct Lyapunov functions [8] and to deal with ubiquitous uncertainties [9], [10].

To overcome the limitations of existing technologies, a reachable set approach is presented to efficiently assess the stability of microgrids with the deep integration of power-electronic-interfaced distributed renewables and loads. The novelties of the reachable set method are threefold:

1) It can directly obtain possible operation ranges for a microgrid system subject to disturbances, rather than repeatedly simulating and analyzing the system with ongoing disturbances.
2) The reachable set results shed light on how different disturbances impact the stability of the microgrid system.
3) The reachable set method can be used to estimate the stability margin of the microgrid system under uncertain conditions.

The remainder of this paper is organized as follows: Section II describes the modeling of a microgrid system and its disturbances. Section III establishes the methodological foundations of reachability analysis. Section IV presents the procedure of calculating a reachable set. In Section V, tests conducted on a typical microgrid verify the feasibility and effectiveness of the presented approach. Conclusions are drawn in Section VI.

II. Modeling of Power-electronics-interfaced Microgrids and Disturbances

A. Modeling of Microgrids

A microgrid system consisting of renewables, power electronic devices, loads, and backbones can be expressed by state and algebraic equations [3]. Mathematically, such a microgrid

This material is based upon work supported by the National Science Foundation under Grant No. 1611095.

978-1-5386-7703-2/18/$31.00 ©2018 IEEE

system can be described by a set of differential-algebraic equations (DAEs) as follows:

$$\begin{cases} \dot{\mathbf{x}} = \mathbf{F}(\mathbf{x}, \mathbf{y}, \mathbf{p}) \\ \mathbf{0} = \mathbf{G}(\mathbf{x}, \mathbf{y}, \mathbf{p}), \end{cases} \tag{1}$$

where $\mathbf{x} \in \mathbb{R}^n$ is the state variable vector, $\mathbf{y} \in \mathbb{R}^m$ is the algebraic variable vector, and $\mathbf{p} \in \mathbb{R}^p$ is the disturbance vector, which will be formulated using a set-based approach. Linearizing the microgrid system at the operation point $(\mathbf{x_0}, \mathbf{y_0}, \mathbf{p_0})$, one can obtain (2), when the partial derivative matrix of algebraic equations with respect to algebraic variables, $\mathbf{G_y}$, is nonsingular.

$$\Delta\dot{\mathbf{x}} = [\mathbf{F_x} - \mathbf{F_y}\mathbf{G_y^{-1}}\mathbf{G_x}]\Delta\mathbf{x} + [\mathbf{F_p} - \mathbf{F_y}\mathbf{G_y^{-1}}\mathbf{G_p}]\Delta\mathbf{p}, \tag{2}$$

where $\mathbf{A}_{MGS} = \mathbf{F_x} - \mathbf{F_y}\mathbf{G_y^{-1}}\mathbf{G_x}$ is the state matrix.

In order to efficiently calculate the state matrix described above, its increment is expressed in the form of sub-matrices. The following (3) is given as an example to show the impact of disturbances from distributed renewables and power loads:

$$\mathbf{A}_{MGS,P} = \sum_{j=1}^{N_G} \mathbf{A}_{G_j} + \sum_{k=1}^{N_L} \mathbf{A}_{L_k} + \sum_{j=1}^{N_G}\sum_{k=1}^{N_L} \mathbf{A}_{G_j,L_k}, \tag{3}$$

where N_G is the number of renewables in the microgrid system, N_L is the number of loads, $\mathbf{A}_{G_j}$ and $\mathbf{A}_{L_k}$ are the increments only correlated to renewables and loads, respectively, and the cross items $\mathbf{A}_{G_j,L_k}$ represent the mutual effects of renewables and loads on the matrix increment. Their expressions are given as follows:

$$\begin{aligned} \mathbf{A}_{G_j} = {} & \mathbf{F}_{\mathbf{x},\mathbf{G_j}} - \mathbf{F}_{\mathbf{y},\mathbf{G_j}}\mathbf{G_y^{-1}}\mathbf{G}_{\mathbf{x},\mathbf{G_j}} - \mathbf{F}_{\mathbf{y},\mathbf{G_j}}\mathbf{G_y^{-1}}\mathbf{G}_{\mathbf{x},\mathbf{C}} \\ & -\mathbf{F}_{\mathbf{y},\mathbf{C}}\mathbf{G_y^{-1}}\mathbf{G}_{\mathbf{x},\mathbf{G_j}}, \end{aligned} \tag{4}$$

$$\begin{aligned} \mathbf{A}_{L_k} = {} & \mathbf{F}_{\mathbf{x},\mathbf{L_k}} - \mathbf{F}_{\mathbf{y},\mathbf{L_k}}\mathbf{G_y^{-1}}\mathbf{G}_{\mathbf{x},\mathbf{L_k}} - \mathbf{F}_{\mathbf{y},\mathbf{L_k}}\mathbf{G_y^{-1}}\mathbf{G}_{\mathbf{x},\mathbf{C}} \\ & -\mathbf{F}_{\mathbf{y},\mathbf{C}}\mathbf{G_y^{-1}}\mathbf{G}_{\mathbf{x},\mathbf{L_k}}, \end{aligned} \tag{5}$$

$$\mathbf{A}_{G_j,L_k} = -\mathbf{F}_{\mathbf{y},\mathbf{G_j}}\mathbf{G_y^{-1}}\mathbf{G}_{\mathbf{x},\mathbf{L_k}} - \mathbf{F}_{\mathbf{y},\mathbf{L_k}}\mathbf{G_y^{-1}}\mathbf{G}_{\mathbf{x},\mathbf{G_j}}, \tag{6}$$

where $\mathbf{F}_{\mathbf{x},\mathbf{G_j}}$, $\mathbf{F}_{\mathbf{y},\mathbf{G_j}}$, $\mathbf{G}_{\mathbf{x},\mathbf{G_j}}$ are matrices only correlated to the uncertainties from the j^{th} renewable, $\mathbf{F}_{\mathbf{x},\mathbf{L_k}}$, $\mathbf{F}_{\mathbf{y},\mathbf{L_k}}$, $\mathbf{G}_{\mathbf{x},\mathbf{L_k}}$ are matrices only correlated to the changes of the j^{th} load, $\mathbf{F}_{\mathbf{y},\mathbf{C}}$ and $\mathbf{G}_{\mathbf{x},\mathbf{C}}$ are constant matrices uncorrelated with any disturbances.

By using the above matrix decomposition, it becomes easy and efficient to calculate $\mathbf{A}_{MGS,P}$ when disturbances occur, because only specific sub-matrices need to be updated.

B. Modeling of Disturbances in Microgrids

Instead of using the traditional point-based methods, a set-based approach, zonotope [11], is adopted to better quantify uncertainties, because a zonotope is computationally both efficient and stable, closed under Minkowski operations, and suitable for convex hull computations and convex optimization. A zonotope $\mathcal{P}$ is defined by a center and generators as follows [11]:

$$\mathcal{P} = \{\boldsymbol{c} + \sum_{i=1}^{m} \beta_i \boldsymbol{g}_i \mid \beta_i \in [-1, 1]\}, \tag{7}$$

where $\boldsymbol{c} \in \mathbb{R}^n$ is the center and $\boldsymbol{g}_i \in \mathbb{R}^n$ are generators.

Therefore, by using (7), the uncertain input $[\mathbf{F_p} - \mathbf{F_y}\mathbf{G_y^{-1}}\mathbf{G_p}]\Delta\mathbf{p}$ in (2) can be expressed in a zonotope. For a more accurate characterization of uncertainties, polynomial zonotypes and probabilistic zonotypes can be used.

III. Reachable Set Algorithm

Reachable set calculation aims at finding the bounds of all possible system trajectories under various disturbances. The calculation process can be presented as follows:

First, the original nonlinear DAEs of a dynamic system are abstracted into linear differential inclusions at each time step, obtaining a finite-dimensional state matrix of the system $\mathbf{A} = [a_{ij}] \in \mathbb{R}^{n\times n}$. Its reachability analysis under uncertainties can then be expressed as follows [12]:

$$\Delta\dot{\mathbf{x}} \in \mathbf{A}\Delta\mathbf{x} \oplus \mathbf{P}, \tag{8}$$

where $\mathbf{A}$ represents the state matrix which is equivalent to $\mathbf{A}_{MGS}$ in (2), $\Delta\mathbf{x} = \mathbf{x} - \mathbf{x_0}$, $\mathbf{x_0}$ is the operation point where the system is linearized, $\mathbf{P}$ is a set of uncertain inputs, and $\oplus$ is Minkowski addition defined as follows by using two sets S and T [11].

$$S \oplus T = \{s + t | s \in S, t \in T\}.$$

Second, a reachable set can be obtained at each time step via a closed-form solution [13]:

$$\mathcal{R}^e(t_{k+1}) = \phi(\mathbf{A}, r)\mathcal{R}^e(t_k) \oplus \Psi(\mathbf{A}, r, \mathbf{p_0}) \oplus I_p^e(\mathbf{p_\Delta}, r), \tag{9}$$

$$\begin{aligned} \mathcal{R}^e(\tau_k) = {} & C(\mathcal{R}^e(t_k), \phi(\mathbf{A}, r)\mathcal{R}^e(t_k) \oplus \Psi(\mathbf{A}, r, \mathbf{p_0})) \\ & \oplus I_p^e(\mathbf{p_\Delta}, r) \oplus I_\xi^e, \end{aligned} \tag{10}$$

where $\mathcal{R}^e(t_{k+1})$ is the reachable set at each time step, $\mathcal{R}^e(\tau_k)$ is the reachable set during time steps, $\phi(\mathbf{A}, r)$ represents how the past reachable set $\mathcal{R}^e(t_k)$ contributes to the current one as shown in (11), $\Psi(\mathbf{A}, r, \mathbf{p_0})$ in (12)and $I_p^e(\mathbf{p_\Delta}, r)$ in (13) represent the incremental changes in the reachable sets caused by deterministic inputs $\mathbf{p_0}$ and uncertain ones $\mathbf{p_\Delta}$, respectively, I_ξ^e represents the incremental changes in the reachable set caused by the curvature of trajectories from t_k to t_{k+1} as shown in (14), $r = t_{k+1} - t_k$ is the time interval, and $C(\cdot)$ represents convex hull calculation. The corresponding expressions are given as follows:

$$\phi(\mathbf{A}, r) = \sum_{i=0}^{\eta} \frac{(\mathbf{A}r)^i}{i!}, \tag{11}$$

$$\Psi(\mathbf{A}, r, \mathbf{p_0}) = \left\{ \sum_{i=0}^{\eta} \frac{\mathbf{A}^i r^{i+1}}{(i+1)!} \oplus \left[X(\mathbf{A}, r)r, X(\mathbf{A}, r)r\right] \right\} \mathbf{p_0}, \tag{12}$$

$$I_p^e(\mathbf{p_\Delta}, r) = \sum_{i=0}^{\eta} \left(\frac{\mathbf{A}^i r^{i+1}}{(i+1)!} \mathbf{p_\Delta} \right) \oplus \left\{ \left[X(\mathbf{A}, r)r, X(\mathbf{A}, r)r\right] \cdot \mathbf{p_\Delta} \right\}, \tag{13}$$

$$I_{\xi}^{e} = \Big\{ \big(I \oplus [X(\mathbf{A},r), X(\mathbf{A},r)]\big) \cdot \mathcal{R}^{e}(t_k) \Big\} \oplus \Big\{ \big(\tilde{I} \oplus [X(\mathbf{A},r)r, X(\mathbf{A},r)r]\big) \cdot \mathbf{p_0} \Big\}, \quad (14)$$

$$X(\mathbf{A},r) = e^{|\mathbf{A}|r} - \sum_{i=0}^{\eta} \frac{(|\mathbf{A}|r)^i}{i!}, \quad (15)$$

$$I = \sum_{i=2}^{\eta} \Big[(i^{\frac{-i}{i-1}} - i^{\frac{-1}{i-1}}) r^i, 0 \Big] \frac{\mathbf{A}^i}{i!}, \quad (16)$$

$$\tilde{I} = \sum_{i=2}^{\eta+1} \Big[(i^{\frac{-i}{i-1}} - i^{\frac{-1}{i-1}}) r^i, 0 \Big] \frac{\mathbf{A}^{i-1}}{i!}. \quad (17)$$

IV. Flowchart of Reachable Set Calculation in Microgrid

The computational flowchart of a reachable set is illustrated in Fig. 1. A microgrid system including branches, transformers, power-electronic interfaces, renewables, and loads is initially modeled, and the dynamics of renewables, loads, and their power-electronic-interfaces is then formulated via a set of differential equations. Finally the microgrid system can be modeled by using (2). After that, power flow is formulated and calculated. Based on this, the system is linearized and reachable sets are calculated via (9) and (10). The calculation process will be terminated when the simulation time ends or the reachable set is excessively conservative. If one of these criteria is satisfied, then the process will stop; otherwise, power flow calculations and reachable set computations should continue.

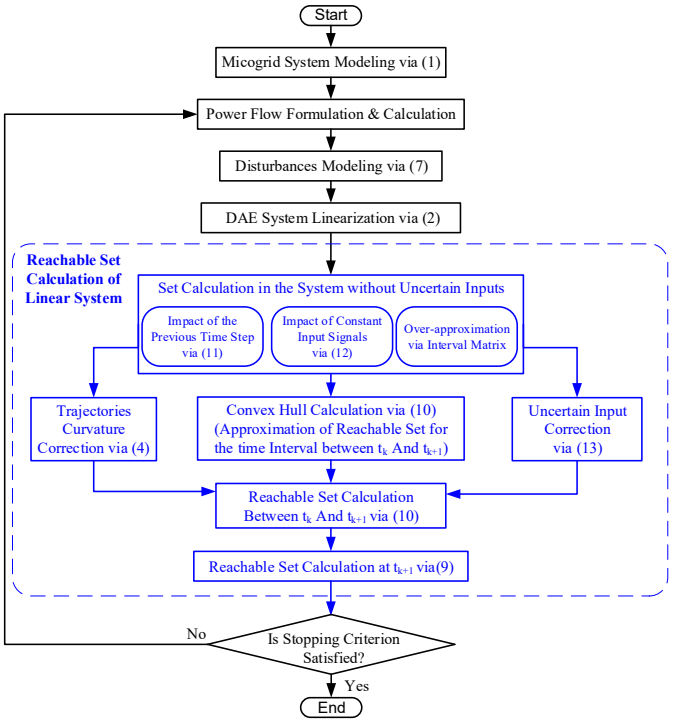

Fig. 1 Flowchart of reachable set calculation

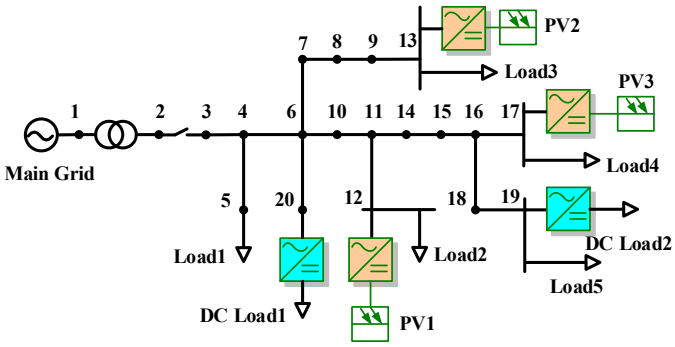

Fig. 2 A microgrid system integrated with power-electronic-interfaced distributed renewables and DC loads.

V. Test Cases

A typical microgrid system that is deeply integrated with distributed renewables and DC power loads shown in Fig. 2 is used to test and validate the presented reachable set approach [14]. The test system includes three PV units and two DC power loads. All five units are integrated into the microgrid via power-electronic interfaces [14]. PV units are controlled via a maximum power point tracking strategy (P&O), whereas DC power loads are controlled using a power output strategy. Thus, uncertainties come from both PVs and DC power loads. Note that the presented approach is developed on the basis of multiple functions in the CORA toolbox [12], [15], and is also potentially applied to a microgrid with ring topology.

A. Reachable Sets under Renewables Uncertainties

In this test, the active power output in PV1 fluctuates around its baseline power by $\pm 1\%$, $\pm 10\%$, and $\pm 25\%$ from the beginning to simulate the changes of irradiance. Under these uncertainties, the reachable sets of X_{pi} and X_{qi} in PV1 and PV3 are given in Fig. 3 and Fig. 4, and Fig. 5 and Fig. 6 show the cross sectional views of reachable set of X_{pi} and X_{qi} along the time line. Here X_{pi}, X_{qi} are the state variables of active and reactive power controllers [3].

- The possible operational range of the microgrid system subject to distributed renewables' disturbances can be directly obtained via reachable set calculation.
- The sizes of the zonotopes along the reachtubes increase as the uncertainty level increases, as the zoomed-in plots in Fig. 3 demonstrate. Its correctness and over-approximation are further demonstrated by the comparison with time domain simulations in the next section.
- The comparison between Fig. 5 and Fig. 6 shows the quantitative differences of the disturbance's impact on PV1 and PV3, respectively. For instance, at 1.5s, the deviations of X_{pi} and X_{qi} in PV1 under 25% disturbance are $[-22.55\%, 19.06\%]$ and $[-183.71\%, 350.42\%]$, whereas those deviations in PV3 are $[-1.55\%, 1.25\%]$ and $[-3.73\%, 2.25\%]$ which are much smaller than those in the PV1, especially the deviations of X_{qi}.

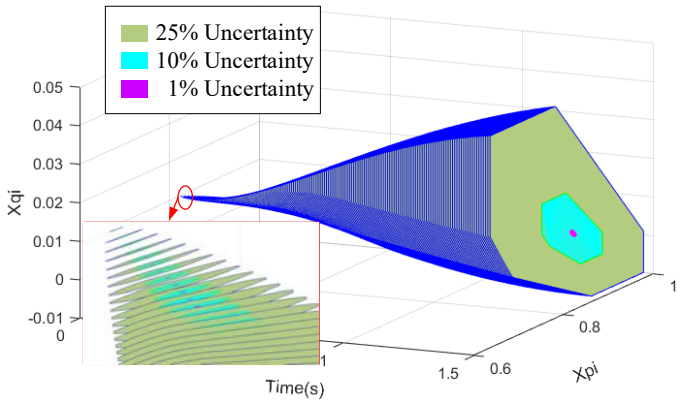

Fig. 3 3-D reachable set of X_{pi}, X_{qi} in PV1

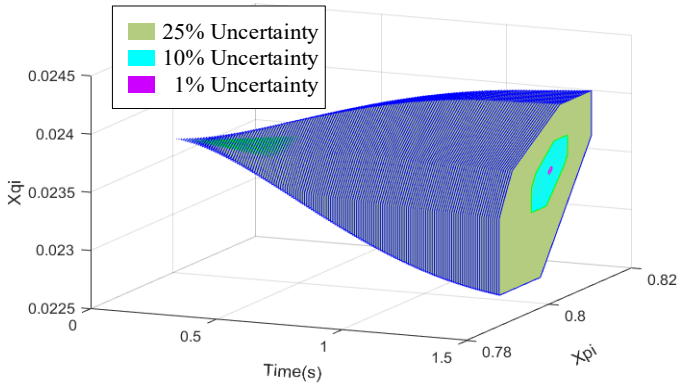

Fig. 4 3-D reachable set of X_{pi}, X_{qi} in PV3

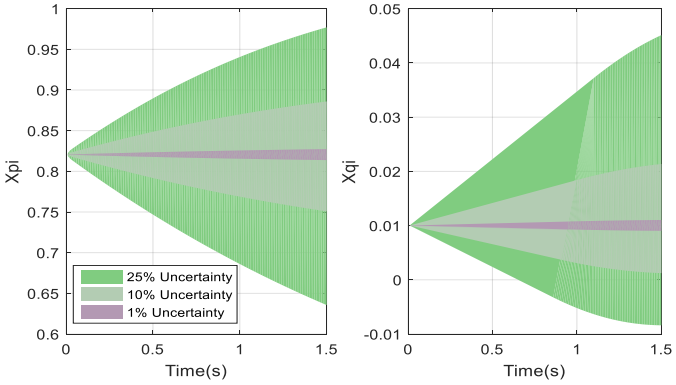

Fig. 5 Reachable set of X_{pi}, X_{qi} in PV1 projected to the time line

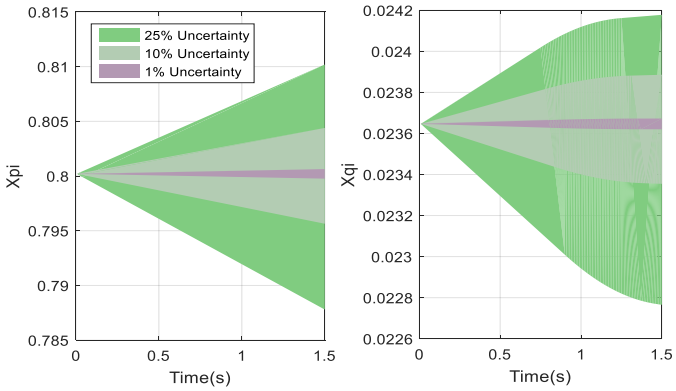

Fig. 6 Reachable set of X_{pi}, X_{qi} in PV3 projected to the time line

B. Reachable Sets under DC Loads Uncertainties

In this test, the DC loads active power fluctuates around the DC loads baseline power at different points in time. For instance, different fluctuations at different points of time shown in Table I are introduced to simulate the changes in DC Load1. Fig. 7 and Fig. 8 offer the following insights:

- The possible operation range of the microgrid system under disturbances from power-electronic interfaced DC loads can be directly obtained via reachable set calculation.
- As the disturbances change along the time line, reachable set results change correspondingly, meaning this method can be used online to provide a real-time evaluation of the system.
- Critical loads can be pinpointed via reachable set results, which enables the system operator to adopt a cost-effective way to improve system performance.

C. Reachable Set Verification via Time Domain Simulations

Time domain simulations are used to validate the effectiveness of reachable sets. For clear illustration, fifteen simulation trajectories are selected to compare against the reachable set results. The fifteen simulation scenarios are summarized in the Appendix. Fig. 9 show the simulation results for X_{pi} and X_{qi} in PV2. The following can be observed from Fig. 9:

- The reachable sets enclose the time domain trajectories, which validates the coverage capability of reachable sets.
- In this test case, the conservatism of reachable sets is acceptable and actually desirable; however, when the distribution system scale increases drastically, techniques to reduce conservatism may become necessary.
- Reachable set calculation time is equivalent to just a few runs of deterministic time domain simulations as shown in Table II, meaning reachable set calculation is efficient.

Table I Fluctuations of DC Load1 at Different Points of Time

Time (s)	0.0	0.2	0.5	0.8	1.1	1.4
Fluctuations (%)	±4.5	±9.4	±19.0	±28.7	±14.6	±9.9

VI. Conclusions

Reachable set calculation is presented as a means of assessing the stability of microgrid systems that are subject to heterogeneous uncertainties due to the high penetration of power-electronic-interfaced distributed renewables and DC loads. With efficient system linearization and zonotope-based disturbances modeling, a mathematically-rigorous reachable

Table II Calculation Times for 1.5s Dynamics on a 3.4GHz PC

Cases \ Uncertainties	25%	10%	1%
Time of Reachable Set Calculation (s)	8.5287	7.6262	7.6025
Time of Fifteen Time Domain Simulations (s)	9.7279	9.6326	9.4852

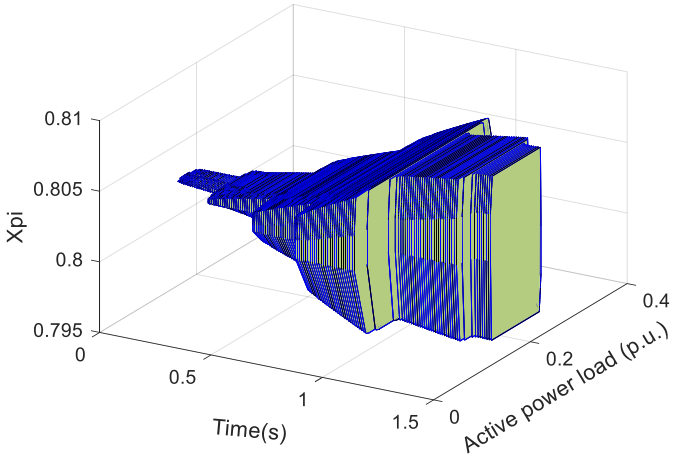

Fig. 7 3-D reachable set of active power load and its control signal of DC Load1

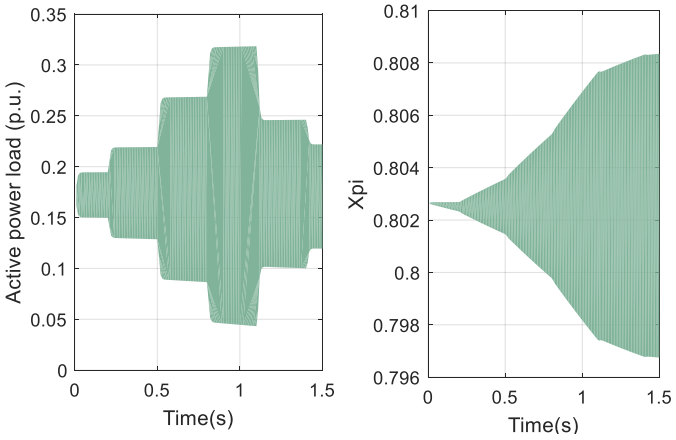

Fig. 8 Reachable set of active power load and its control signal of DC Load1 projected to the time line

set can be calculated along the time line which shows system performance under various disturbances. Numerical tests are performed on a typical microgrid system integrated with renewables and DC loads. Analyses and tests have confirmed the feasibility and effectiveness of reachable set results.

APPENDIX

Table III Fifteen Simulation Scenarios

Time (s)	0.00	0.00	0.10	0.20	0.20
PV1 Uncertainties (%)	20.00	−25.00	−6.50	7.50	25.00
Time (s)	0.30	0.30	0.35	0.40	0.40
PV1 Uncertainties (%)	5.00	25.00	−25.00	−10.00	−25.00
Time (s)	0.50	0.60	0.80	0.90	1.30
PV1 Uncertainties (%)	−20.00	15.00	−15.00	10.00	−17.50

ACKNOWLEDGMENT

The authors would like to thank Matthias Althoff from Technische Universität München, Germany, for the helpful discussion. The authors also would like to thank the anonymous reviewers for the valuable comments.

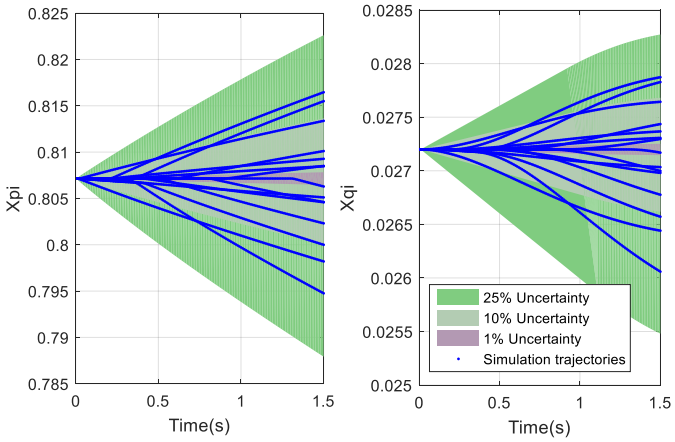

Fig. 9 Time domain simulation verification of PV2

REFERENCES

[1] G. Pepermans, J. Driesen, D. Haeseldonckx, R. Belmans, and W. Dhaeseleer, "Distributed generation: definition, benefits and issues," *Energy policy*, vol. 33, no. 6, pp. 787–798, 2005.

[2] Y. Li, P. Zhang, L. Zhang, and B. Wang, "Active synchronous detection of deception attacks in microgrid control systems," *IEEE Transactions on Smart Grid*, vol. 8, no. 1, pp. 373–375, 2017.

[3] C. Wang, Y. Li, K. Peng, B. Hong, Z. Wu, and C. Sun, "Coordinated optimal design of inverter controllers in a micro-grid with multiple distributed generation units," *IEEE Transactions on Power Systems*, vol. 28, no. 3, pp. 2679–2687, 2013.

[4] N. Duan and K. Sun, "Power system simulation using the multistage adomian decomposition method," *IEEE Transactions on Power Systems*, vol. 32, no. 1, pp. 430–441, 2017.

[5] H.-D. Chang, C.-C. Chu, and G. Cauley, "Direct stability analysis of electric power systems using energy functions: theory, applications, and perspective," *Proceedings of the IEEE*, vol. 83, no. 11, pp. 1497–1529, 1995.

[6] C. Canizares, T. Fernandes, E. Geraldi, L. Gerin-Lajoie, M. Gibbard, I. Hiskens, J. Kersulis, R. Kuiava, L. Lima, F. DeMarco, *et al.*, "Benchmark models for the analysis and control of small-signal oscillatory dynamics in power systems," *IEEE Transactions on Power Systems*, vol. 32, no. 1, pp. 715–722, 2017.

[7] T.-E. Huang, Q. Guo, and H. Sun, "A distributed computing platform supporting power system security knowledge discovery based on online simulation," *IEEE Transactions on Smart Grid*, vol. 8, no. 3, pp. 1513–1524, 2017.

[8] H.-D. Chiang, F. Wu, and P. Varaiya, "Foundations of direct methods for power system transient stability analysis," *IEEE Transactions on Circuits and Systems*, vol. 34, no. 2, pp. 160–173, 1987.

[9] C. Juarez and A. Stankovic, "Contraction analysis of power system dynamics using time-varying omib equivalents," in *Power Symposium, 2007. NAPS'07. 39th North American*, pp. 385–391, IEEE, 2007.

[10] A. Papachristodoulou and S. Prajna, "Analysis of non-polynomial systems using the sum of squares decomposition," in *Positive Polynomials in Control*, pp. 23–43, Springer, 2005.

[11] M. Althoff and B. H. Krogh, "Zonotope bundles for the efficient computation of reachable sets," in *Decision and Control and European Control Conference (CDC-ECC), 2011 50th IEEE Conference on*, pp. 6814–6821, IEEE, 2011.

[12] Y. Li, P. Zhang, and P. B. Luh, "Formal analysis of networked microgrids dynamics," *IEEE Transactions on Power Systems*, 2017.

[13] M. Althoff, "Formal and compositional analysis of power systems using reachable sets," *IEEE Transactions on Power Systems*, vol. 29, no. 5, pp. 2270–2280, 2014.

[14] S. Papathanassiou, N. Hatziargyriou, K. Strunz, *et al.*, "A benchmark low voltage microgrid network," in *Proceedings of the CIGRE Symposium: Power Systems with Dispersed Generation*, pp. 1–8, 2005.

[15] M. Althoff, "CORA 2016 manual," 2016.